Journal of proteome research

Article

pubs.acs.org/jpr

Involvement of GABA Transporters in Atropine-Treated Myopic Retina As Revealed by iTRAQ Quantitative Proteomics

Veluchamy A. Barathi,[†,‡,§,▽] Shyam S. Chaurasia,[†,‡,§,▽] Michael Poidinger,[∥] Siew Kwan Koh,[†] Dechao Tian,[⊥] Candice Ho,[†] P. Michael Iuvone,[#] Roger W. Beuerman,[†,‡,§] and Lei Zhou*[,†,‡,§]

[†]Singapore Eye Research Institute, 11 Third Hospital Avenue, Singapore 168751, Singapore

[‡]Dept. of Ophthalmology, Yong Loo Lin School of Medicine, National University of Singapore, 5 Lower Kent Ridge Road, Singapore 119074, Singapore

[§]SRP Neuroscience and Behavioral Disorder, DUKE-NUS Graduate Medical School, 8 College Road, Singapore 169857, Singapore

[∥]Singapore Immunology Network, A*Star, 8a Biomedical Grove, Singapore 138648, Singapore

[⊥]Department of Statistics and Applied Probability, National University of Singapore, 6 Science Drive 2, Singapore 117546, Singapore

[#]Departments of Ophthalmology and Pharmacology, Emory University School of Medicine, 1365B Clifton Road NE, Atlanta, Georgia 30322, United States

Supporting Information

ABSTRACT: Atropine, a muscarinic antagonist, is known to inhibit myopia progression in several animal models and humans. However, the mode of action is not established yet. In this study, we compared quantitative iTRAQ proteomic analysis in the retinas collected from control and lens-induced myopic (LIM) mouse eyes treated with atropine. The myopic group received a (−15D) spectacle lens over the right eye on postnatal day 10 with or without atropine eye drops starting on postnatal day 24. Axial length was measured by optical low coherence interferometry (OLCI), AC-Master, and refraction was measured by automated infrared photorefractor at postnatal 24, 38, and 52 days. Retinal tissue samples were pooled from six eyes for each group. The experiments were repeated twice, and technical replicates were also performed for liquid chromatography−tandem mass spectrometry (LC−MS/MS) analysis. MetaCore was used to perform protein profiling for pathway analysis. We identified a total of 3882 unique proteins with <1% FDR by analyzing the samples in replicates for two independent experiments. This is the largest number of mouse retina proteome reported to date. Thirty proteins were found to be up-regulated (ratio for myopia/control > global mean ratio + 1 standard deviation), and 28 proteins were down-regulated (ratio for myopia/control < global mean ratio - 1 standard deviation) in myopic eyes as compared with control retinas. Pathway analysis using MetaCore revealed regulation of γ-aminobutyric acid (GABA) levels in the myopic eyes. Detailed analysis of the quantitative proteomics data showed that the levels of GABA transporter 1 (GAT-1) were elevated in myopic retina and significantly reduced after atropine treatment. These results were further validated with immunohistochemistry and Western blot analysis. In conclusion, this study provides a comprehensive quantitative proteomic analysis of atropine-treated mouse retina and suggests the involvement of GABAergic signaling in the antimyopic effects of atropine in mouse eyes. The GABAergic transmission in the neural retina plays a pivotal role in the maintenance of axial eye growth in mammals.

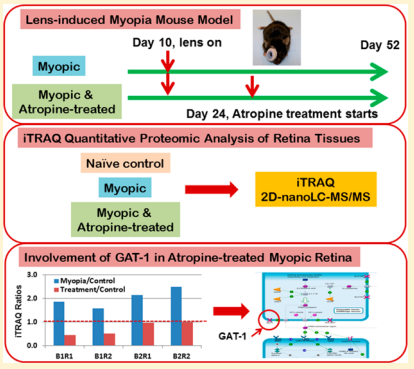

KEYWORDS: *retina proteomics, iTRAQ, quantitative proteomics, myopia, lens-induced myopia mouse model*

INTRODUCTION

Myopia (near-sightedness) is the leading cause of visual disability throughout the world.[1−4] It is a common condition usually caused by excessive elongation of eyeball where the focal point of the eye lies in front of the retina, making distant objects difficult to focus. In the U.S. and Europe, the prevalence of myopia ranges from 25 to 40%, whereas in Asian countries it has been reported as high as 80−90%.[3,5,6]

Several strategies have been employed to slow down or inhibit the progression of myopia in humans.[7] These include bifocals, multifocal, and under-correction contact lenses; however, no long-term substantial treatment method with acceptable side effects has been found yet. Of all methods, the use of Atropine eye drops, a pan muscarinic receptor antagonist, has had the most effective results seen to halt the progression of childhood myopia.[8] This was followed by several clinical trials, where atropine (0.01 to 1%) was found to be effective in inhibiting the progression of myopia.[9−11] To date, atropine remains the most

Special Issue: Proteomics of Human Diseases: Pathogenesis, Diagnosis, Prognosis, and Treatment

Received: June 6, 2014
Published: September 11, 2014

   dx.doi.org/10.1021/pr500558y | J. Proteome Res. 2014, 13, 4647−4658

effective intervention to prevent myopia with unknown mechanism.

The mechanism of atropine action in the treatment of myopia and its potential contribution in axial elongation has been a subject of interest for scientists in the past decade.[11,12] Retinal participation in the regulation of postnatal eye growth has been investigated,[13,14] and it was suggested that neurotransmitters, such as vasoactive intestinal polypeptide (VIP), dopamine,[14] acetylcholine,[15] and γ-aminobutyric acid (GABA),[16,17] may act directly on the sclera or trigger the release of growth factors from retina that modulate scleral growth. Recent biochemical and pharmacological studies suggest that retinal dopaminergic and GABAergic neurotransmitter systems play a substantial role in the modulation of eye growth and refractive development in animals.[17−19] Previous studies have shown that dopamine via D2 receptors controls eye growth in animals.[18,19] A recent study showed that GABAergic agonists inhibit the protective effect of brief periods of normal vision on the development of form-deprivation myopia, whereas antagonists enhanced the protective effects.[17] Moreover, GABA receptor agonists decrease dopamine release in the retina.[20,21] Thus, these studies suggest that dopaminergic neurons exert their effects on the eye growth via interacting with GABAergic pathway. Despite these efforts, the messengers released by the retina to induce these changes are still largely unknown.

Proteomic approaches have been used to study retina and sclera tissues in a chick model,[22,23] scleral tissue in tree shrew,[24,25] retinal, retinal pigment epithelium (RPE), and choroidal tissues in tilapia,[26] and scleral tissue in a guinea pig model.[27] Aqueous humor samples from patients with myopia were also examined using proteomic analysis.[28] However, the comprehensive retinal proteome in mouse myopic eyes has not been reported yet. The purpose of the present study is to establish quantitative mouse retinal proteome and study the differences between the lens-induced myopia (LIM) and atropine-treated LIM retinal proteomes. Identification of myopia-susceptible proteins will provide valuable insight into the molecular basis of this eye disorder and help identify pathways that are involved in eye growth and development. These efforts may lead to the development of potential therapeutic strategies to tackle this preventable blinding disorder.

METHODS

Reagents

Sucrose, tris (hydroxymethyl) aminomethane, magnesium chloride, glucose, 3-[(3-cholamidopropyl) dimethylammoniol-1-propanesulfonate (CHAPS), and ammonium bicarbonate were purchased from Sigma-Aldrich (St. Louis, MO). EDTA-free Halt Cocktail Protease inhibitor was purchased from Thermo Fisher Scientific, USA. HPLC-grade acetonitrile (ACN), formic acid (FA), and water were obtained from Merck (Darmstadt, Germany). Rabbit polyclonal antibodies to GABA transporter 1 (GAT-1), myelin expression factor2 (MYEF2), and rabbit monoclonal antibodies to isoform 1 of syntaxin-binding protein 1 (STXBP1) were purchased from Abcam, Cambridge, U.K.

Animals

C57BL/6 mice (n = 45) were obtained from the animal holding unit of the National University of Singapore. All animals were housed in standard mouse cages at 25 °C on a schedule of 12 h: 12 h of light (325 lx) and dark cycle (0 lx) with mouse pellet and water available ad libitum. SingHealth Institutional Animal Care and Use Committee (IACUC) approved all of the procedures performed in this study and were in accordance with the Guide for the Care and Use of Laboratory Animals.

Lens-Induced Myopia (LIM) and Atropine Treatment

The experimental design is illustrated in Figure 1. C57BL/6 mice were divided into three groups. The groups were divided into myopic group, atropine-treated group, and age-matched naïve control group. The hard lens was placed over the right eye of two groups of (three batches, six animals per batch in each group) mice on day 10 and remained in place until postnatal day 52. Briefly, the lens was attached by gluing a negative (−15 D) contact lens with 8.5 mm diameter and 8 mm base curve to an annulus of Velcro (PMMA Spectacle Lens in Blue Tint, refractive index: 1.43, lens thickness: 0.5 mm, radius of outer curvature: 8.5 mm, and inner curvature: 8 mm, Lenspec Technology Pte, Singapore). This mating piece was then attached to the Velcro that had been previously cemented to the hair around the eye using a nitrocellulose solution (collodion USP, Fisher Scientific, NJ). The spectacle lenses were cleaned daily under red light. An air gap was recognized to exist between the back surface of the lens and the anterior surface of the cornea of 1.5 mm, and thus the contact lens optically acted like a spectacle lens. The left eyes were uncovered and served as contralateral fellow eyes. One of the myopic groups received one drop of 1% atropine sulfate topically. The treatment was started on postnatal day 24. Axial length and refractive error measurements were measured every week, as previously described.[29−32] Two batches (30 mice) were used for proteomic analysis, and another batch (15 mice) was reserved for verification of proteomic results using Western blot and immunohistochemistry. The anesthetized mice were euthanized by overdose of pentobarbitol sodium (85 mg/kg body weight, I/P injection); then, immediately, eyes were enucleated, which were kept under cold 1× PBS solution. Briefly, under a dissecting microscope an incision was made at the

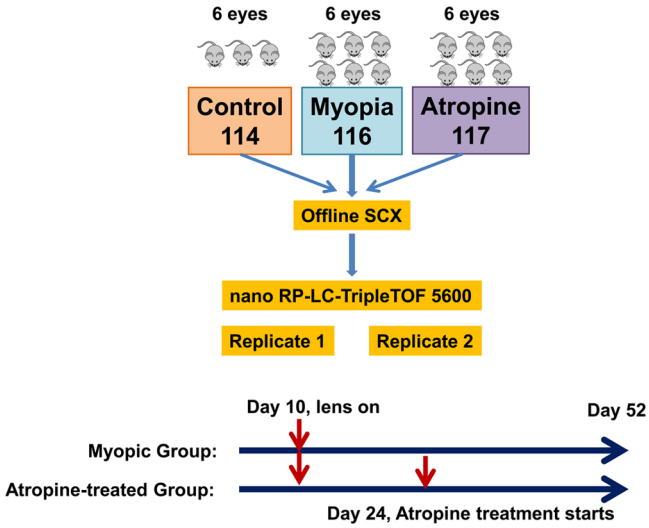

Figure 1. Experimental design for iTRAQ-based quantitative proteomic analysis. The whole experiment was repeated (two batches) and each SCX fraction was analyzed twice using nanoRP-LC−MS/MS (Replicates 1 and 2). Thus, there are two biological replicates and two technical replicates. The hard lenses were placed over the right eye of mice from two groups (myopic group and atropine-treated group) on day 10 and remained in place until postnatal day 52. Atropine-treated group received one drop of 1% atropine sulfate topically. The treatment was started on postnatal day 24.

dx.doi.org/10.1021/pr500558y | J. Proteome Res. 2014, 13, 4647−4658

limbus, and the cornea was dissected from the sclera. The lens was gently removed without disturbing the retina. The full extent of the retina was gently dissected from the sclera using fine forceps; then, the retina was frozen immediately in liquid nitrogen. The retina was stored at −80 °C for further analysis. The whole process was done within 5 min per mouse.

Retinal Protein Extraction, Digestion and iTRAQ Labeling

Retina samples were pooled from six eyes in LIM group, atropine-treated LIM group, and control group for proteomic analysis. Retina tissues were suspended in 1.5 volume of lysis buffer solution [20% sucrose, 20 mM Tris (hydroxymethyl)-aminomethane, 2 mM magnesium chloride, 10 mM glucose, and 2% 3-[(3-cholamidopropyl) dimethylammoniol-1-propanesulfonate (CHAPS)] at pH 7.2 and 1.3 volume of EDTA-free Halt Cocktail Protease inhibitor. The samples were subjected to 10 times freeze−thaw cycle in liquid nitrogen, followed by homogenization using a mortar and pestle for 1 min.[33] Samples were centrifuged at 6000 rcf for 10 min at 4 °C, and supernatants were collected. The pellets were sonicated in 20 μL of lysis buffer for 30 s at 0 °C and centrifuged. Supernatants were combined. Six volumes of cold acetone (Pierce, USA) were added to 150 μg of each sample and mixed well prior to overnight incubation at −30 °C. Samples were then centrifuged at 16,000 rcf for 10 min at 4 °C to pellet the protein precipitates. The supernatants were decanted, and pellets were resolubilized in 100 μL of 50 mM ammonium bicarbonate buffer at pH 7.4. 100 μg of each sample was transferred into new tubes and dried using SpeedVac (Thermo Fisher Scientific, USA). Total concentration of extracted proteins was determined using DC Protein Assay Solutions (Bio-Rad, USA).

Reagents and buffers for iTRAQ experiments were obtained from the iTRAQ Reagent Multiplex Kit (AB SCIEX, USA). Protein samples were resolubilized in 20 μL of dissolution buffer (0.5M triethylammoniumbicarbonate (TEAB)), denatured using 1 μL of 2% sodium dodecyl sulfate (SDS), and reduced by 2 μL of reducing reagent (tris(2-carboxyethyl) phosphine (TCEP)). After 1 h of incubation at 60 °C, the protein cysteine residue was blocked by the addition of 1 μL of MMTS at room temperature (RT) for 20 min. The resulting protein samples were digested with trypsin (AB SCIEX, USA) at a substrate/enzyme ratio of 10:1 for 16 h with gentle shaking at 37 °C. iTRAQ reagents were then added to the solution according to the manufacturer's protocol in the following manner: iTRAQ Reagent 114 to nonmyopic native control, 116 to lens-induced myopic, and 117 to atropine-treated myopic peptide sample. After 3 h of incubation at 25 °C, the contents of each iTRAQ reagent labeled samples were combined and dried using SpeedVac to a volume of approximately 100 μL for peptide fractionation.

Offline SCX Fractionation

iTRAQ-labeled peptide samples were fractionated by SCX chromatography using Waters 2695 separation module coupled to Waters photodiode array detector. A silica-based, polysulfethyl column (The Nest Group, USA) of parameters 2.1 mm i.d × 100 mm, 5 μm, 200 Å was used. The binary mobile phase systems were prepared as follows: Buffer A (0.26 M FA, 10% ACN) and Buffer B (0.5 M ammonium formate, 0.26 M FA, 10% ACN). The dried sample was reconstituted with Buffer A to 100 μL and loaded into the high-performance liquid chromatography (HPLC) system for peptide fractionation. A 60 min gradient was performed for Buffer B, from 0 to 100% at a flow rate of 0.2 mL/min. Sixty fractions were collected for 1 min per fraction. Some fractions were combined to yield 35 fractions in total. Each fraction was then cleaned up using UltraMicroSpin Column, Silica C18 (The Nest Group, USA), dried using SpeedVac, and reconstituted with 10 μL of loading buffer (0.1% FA, 2% ACN) for nanoRPLC−ESI−MS/MS analysis.

nanoRPLC−ESI−MS/MS

SCX fractions were subjected to analysis by online 1D nanoRPLC−ESI−MS/MS using a high-resolution Triple TOF 5600 mass spectrometer (AB SCIEX, USA). An RP monolithic capillary high-resolution LC column (100 μm i.d × 15 cm; Merck, Germany) was used for LC separation of peptides. Samples were first loaded onto a Reprosil trapping cartridge (C18-AQ, 150 μm × 5 μm, 120 Å) (SGE Analytical Science, Australia) from a Famos autosampler (Dionex, USA) at 20 μL/min for desalting. After washing with 0.1% FA in HPLC-grade water for 5 min, the system was switched (Switchos, Dionex, USA) into line with the RP analytical capillary column. The tryptic digest was analyzed using an ultimate solvent delivery system (Dionex, USA), with 1 h four-step gradient (ACN in 0.1% FA from 5 to 22% over 38 min, 22 to 40% over 18 min, 40 to 60% over 5 min, 60 to 90% in 1 min and kept at 90% for 5 min) at a flow rate of 300 nL/min. Key parameter settings for the TripleTOF 5600 mass spectrometer were as follows: ionspray voltage floating (ISVF) 2700 V, curtain gas (CUR) 30, interface heater temperature (IHT) 150, ion source gas 1 (GS1) 13, and declustering potential (DP) 80 V.

Data were acquired using information-dependent acquisition (IDA) mode with Analyst TF 1.5 software (AB SCIEX, USA). For IDA parameters, 0.25 s MS survey scan in the mass range of 350−1250 was followed by 20 MS/MS scans of 100 ms in the mass range of 100−1800 (total cycle time: 2.25 s). Switching criteria were set to ions greater than mass-to-charge ratio (m/z) 350 and smaller than m/z 1250 with charge state of 2−5 and an abundance threshold of more than 100 counts. Former target ions were excluded for 8 s. IDA rolling collision energy (CE) parameters script was used for automatic controlling the CE.

Data Processing

ProteinPilot software version 4.01 (AB SCIEX, USA) was used to analyze the MS/MS data output and searched against the International Protein Index (IPI) protein mouse database version 3.77 for protein identification (115 194 proteins searched). "Reversed Protein Sequences" was set for the ProteomicS Performance Evaluation Pipeline (PSPEP) software (AB SCIEX, USA). Other important settings in the Paragon search algorithm in ProteinPilot were configured as follows: (1) Sample type: iTRAQ 4plex (peptide labeled); (2) Cys alkylation: MMTS; (3) Digestion: trypsin; (4) Instrument: TripleTOF 5600; (5) Special factors: none; (6) ID Focus: Biological modifications; (7) Search effort: Thorough ID; and (8) bias correction and background correction were applied. 95% confidence level was used at the peptide level. False discovery rate (FDR) analysis in the ProteinPilot software was performed, and FDR < 1% was set for protein identification. Reverse database search strategy was used to calculate FDR for peptide identification. The data from all fractions were combined as a batch and used for protein identification and relative quantification using ProteinPilot. For relative quantification, ProteinPilot software uses Pro Group algorithm to calculate the reporter ions' peak area. Auto bias correction was applied to eliminate possible pipetting error during the combination of differentially labeled samples.

Bioinformatic Analysis

Functional analysis of Gene Ontology (GO) annotations of the identified retinal proteins was performed using DAVID (Database for Annotation, Visualization and Integrated Discovery, version 6.7) tool.[34,35] The pie charts for Cellular Component, Biological Process, and Molecular Function were generated based on the percentage contribution of each annotation cluster. All proteins differentially expressed were clustered according to their expression profiles in myopia versus treatment using the Short Time-series Expression Miner (STEM),[36] using the STEM clustering method, as outlined in the paper. Proteins from selected profiles were then analyzed for pathway enrichment using MetaCore from GeneGo. To perform pathway analysis, we used "Pathway Maps" under page "one-click analysis" in MetaCore.

Immunohistochemistry

Immunohistochemistry (IHC) was performed on mouse eyes for the expression of GAT-1 proteins. Briefly, whole mouse eyes (6 weeks LIM, atropine-treated LIM, and naïve control eyes) were embedded in Optimal Cutting Temperature (OCT) compound at −20 °C and stored at −80 °C until used in the experiments. Prepared tissue blocks were sectioned with a cryostat at 6 μm thickness and collected on clean polysine microscope glass slides (Gerhard Menzel, Thermo Fisher Scientific, Newington, CT). Slides with the sections were air-dried at RT for 1 h. A standard procedure for hematoxylin and eosin staining was performed as previously mentioned.[31]

Immunofluorescence staining was performed on the sections fixed with 4% paraformaldehyde for 10 min. After washing three times with 1× PBS for 5 min, 4% bovine serum albumin (BSA) in 0.1% Triton X-100 and 1× PBS were added as a blocking buffer. The slides were then covered and incubated for 1 h at RT in a humid chamber. After rinsing with 1× PBS, a specific primary antibody raised in rabbit against GAT-1 (1:80) antibody was diluted with 4% BSA and incubated at 4 °C in a humid chamber overnight. After washing two times with 1× PBS and once with 0.1% Tween-20 for 10 min, Alexa Fluoro 488-conjugated fluorescein-labeled goat antirabbit IgG secondary antibody (Invitrogen, Eugene, OR) was applied at a concentration of 1:800 in 1× PBS with 0.1% Triton X-100 and incubated for 90 min at RT. After washing and air-drying, slides were mounted with antifade medium containing DAPI (4,6-diamidino-2-phenylindole; Vectashield, Vector Laboratories, Burlingame, CA) to visualize the cell nuclei. A fluorescence microscope (Axioplan 2; Carl Zeiss Meditec, Oberkochen, Germany) was used to examine the slides and capture images. Experiments were repeated in duplicates from three different independent samples.

Western Blot

Western blot was performed on retinal samples to further validate the iTRAQ results. Total protein concentration was determined using a direct colorimetric protein assay reagent (Bio-Rad, USA). Twenty micrograms of retinal protein sample was separated on 10% SDS-PAGE and transferred to nitrocellulose membranes. The membrane was blocked in 5% milk for 1 h and washed briefly with TBS-Tween (10 mM Tris-HCl [pH 8.0], 150 mM NaCl, and 0.05% Tween-20). It was then incubated with primary antibody GAT-1, MYEF2, and STBXP1 that were raised in rabbit (Abcam, U.K.) at a dilution of 1:2000, 1:1000, and 1:6000, respectively, in 1× PBS for 3 h followed by three 10 min washes with TBS-Tween. Secondary antirabbit antibody (antirabbit IgG HRP; Thermo Fisher Scientific) was then added at a dilution of 1:1000 in 1× PBS for 1 h, followed by three 5 min washes. β-Tubulin (Sigma-Aldrich, St. Louis, MO) was used as a loading control. Protein bands were visualized using the enhanced chemiluminescence method (GE Healthcare, Buckinghamshire, U.K.) and quantified with Quantity One (Bio-Rad, USA).

RESULTS

Refraction and Axial Length Changes

Right and left eyes of the three age-matched naïve control groups did not differ significantly in any of the experiments performed; therefore, the right and left eye values were averaged. Similar to animals examined in previous studies, the eyes of these three naïve control groups were hyperopic.[29,31,32] Their refractions (corrected for the small eye "artifact")[37] were hyperopic at 52 days (Figure 2A). The axial length of these three groups was not statistically significant (one-way ANOVA; n = 18 eyes; p = 0.28; Figure 2B).

The refraction in eyes with minus lenses alone were −6.3D ± −1.14D (mean ± SD) with an axial length of 3.72 mm ±0.07 mm, while the refraction in fellow eyes was 6.8D ± 1.02D and axial length was 3.37 mm ±0.09 mm (n = 18, p = 0.000054, and p = 0.000022, respectively). The refraction was shifted from myopic to hyperopic after receiving the atropine treatment, and axial length was similar to naïve control group (5.1D ± 2.12D and p = 0.00082; 3.42 ±0.06 mm and p = 0.00011; n = 18 eyes in each group; Figure 2).

Mouse Retinal Proteome

To minimize the biological variation among mice, we pooled the retina tissues from six eyes for each group (i.e., control, myopic, and atropine-treated). The whole experiment was repeated twice (two batches). Furthermore, each SCX fraction was analyzed twice to minimize the technical variations. We identified 3151 (2626 proteins identified with ≥2 peptides) and 2959 (2355 proteins identified with ≥2 peptides) unique proteins from Batch 1 and Batch 2, respectively (<1% FDR). By combining data from two batches (Figure 3), a total of 3882 unique proteins were identified with <1% FDR (using built-in FDR analysis in ProteinPilot software). A total of 2228 proteins (57%) were found in common from batch 1 and batch 2, probably due to the heterogenic complexity of the retina tissue samples. By analyzing the samples in replicates for two independent experiments (Batch 1 and Batch 2), we were able to enhance the coverage of the mouse retina proteome, which represents the largest number of mouse retina proteome reported to date. Table 1 listed the number of spectra used for identification, number of unique peptides identified, number of unique proteins identified and number of unique proteins identified based on no fewer than two peptides. The complete list of 3882 unique proteins identified from mouse retina is provided as Supporting Information (Supplementary Table 1). GO annotation analysis was subsequently performed for these identified retina proteins using DAVID tool. Pie charts representing three GO categories (i.e., Cellular Component, Biological Process, and Molecular Function) are described in Supplemental Figure 1 in the Supporting Information.

Relative Quantification of Retina Proteome in Lens-Induced Myopia Mouse Model with or without Atropine Treatment

Among 3882 retina proteins, 3291 proteins can be quantified (2831 proteins quantified with two or more peptides, Supplemental Table 2 in the Supporting Information). The workflow for the entire quantitative analysis of the iTRAQ results

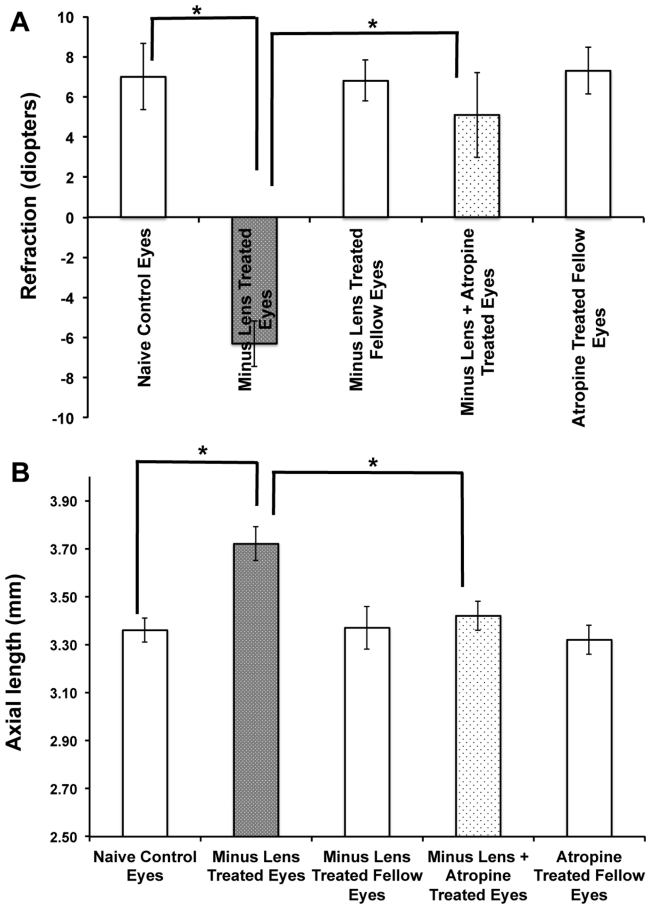

Figure 2. Atropine sulfate (pan muscarinic antagonist) and minus lens-treated B6 mice ocular biometry measurements were plotted against induction period (weeks). This graph represents the ocular biometry of C57BL/6 (B6) mice with −15 D spectacle lens alone or −15 D spectacle lens with atropine treatment. The lens was applied at postnatal day 10 (before eye opening), and the drug treatment was started after 2 weeks of minus lens wearing. The ocular biometry measurements were measured using OLCI-AcMaster (in vivo: accuracy ±10 μm), and refraction (diopters) was measured by automated infrared photorefractor at 2, 4, and 6 weeks after induction of myopia. The refraction (A) and axial length (B) changes were significant after 4 weeks and 6 weeks of myopia induction. Spectacle lens treatment induced myopia and caused elongation of the globe. However, the axial length was significantly reduced after receiving atropine. The lens-treated eyes that received atropine were shifted from myopic to hyperopic refractions, similar to those of naïve control eyes. There was no significant difference seen in the control and fellow eyes. Data were represented as mean ± S.D.; * represents significance level $p < 0.01$.

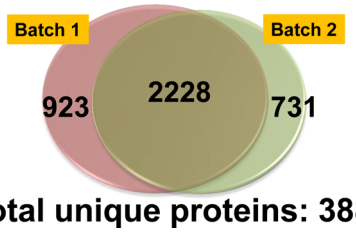

Figure 3. Mouse retinal proteome. In total, 3882 unique proteins were identified with high confidence (<1% FDR) in this study.

is illustrated in Figure 4. Briefly, data with CV% >30% from two technical runs were removed, and iTRAQ ratios from Run1 and Run2 were used to calculate the geometric mean as the final ratio

Table 1. Summary of Four LC−MS/MS Runs (Two Biological Replicates and Two Technical Replicates)

analysis	no. spectra used	no. unique peptide	no. unique protein	no. unique protein (≥2 peptides)
batch1, run1	161811	32097	2583	2194
batch1, run2	118063	25713	2400	1975
batch2, run1	102264	24721	2340	1926
batch2, run2	92521	23353	2390	1888

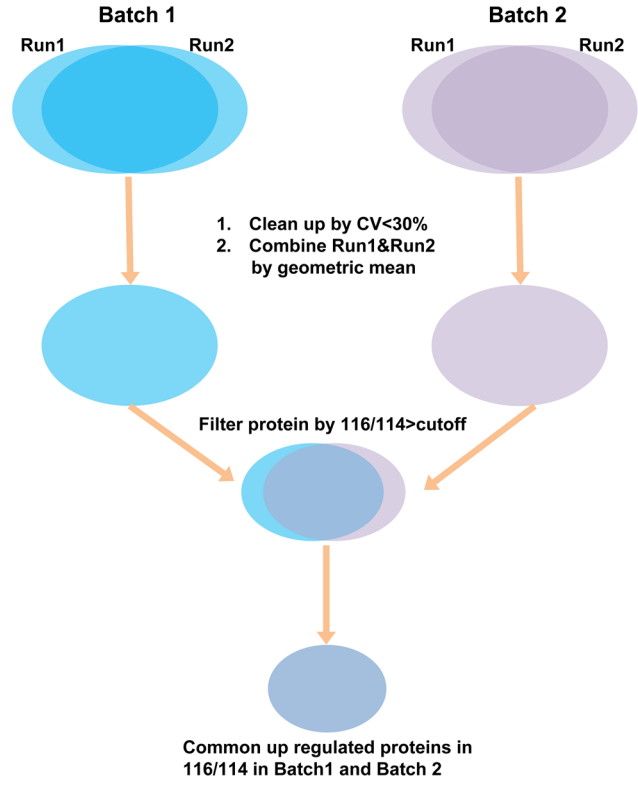

Figure 4. Flowchart shows the iTRAQ data processing.

for each protein. The global mean ratio and standard deviation for the whole data set were determined, and one standard deviation (SD) of the global mean ratio was defined as the cutoff for differentially expression (global mean ratio ±1 SD).[38,39] Only those proteins in common for Batch1 and Batch2 were listed as differentially expressed proteins between myopic group and control group. The same criteria was used for myopic group and atropine group when we determined whether those protein levels were in response to the atropine treatment. Thirty proteins were found to be up-regulated (ratio for myopia/control > global mean +1 SD, Supplemental Table 3A in the Supporting Information), and 28 proteins were down-regulated (ratio for myopia/control < global mean −1 SD, Supplemental Table 3B in the Supporting Information) in all four runs (two biological replicates and two technical replicates) in myopic eyes as compared with control eyes. The changes of retina protein profiles between myopia and atropine treated myopic groups were revealed by Expression Miner software and as described in Figure 5. Using control as the baseline, 13 retina proteins were up-regulated in myopia but were found to be down-regulated (ratio for treatment/myopia < global mean −1 SD) after

dx.doi.org/10.1021/pr500558y | J. Proteome Res. 2014, 13, 4647−4658

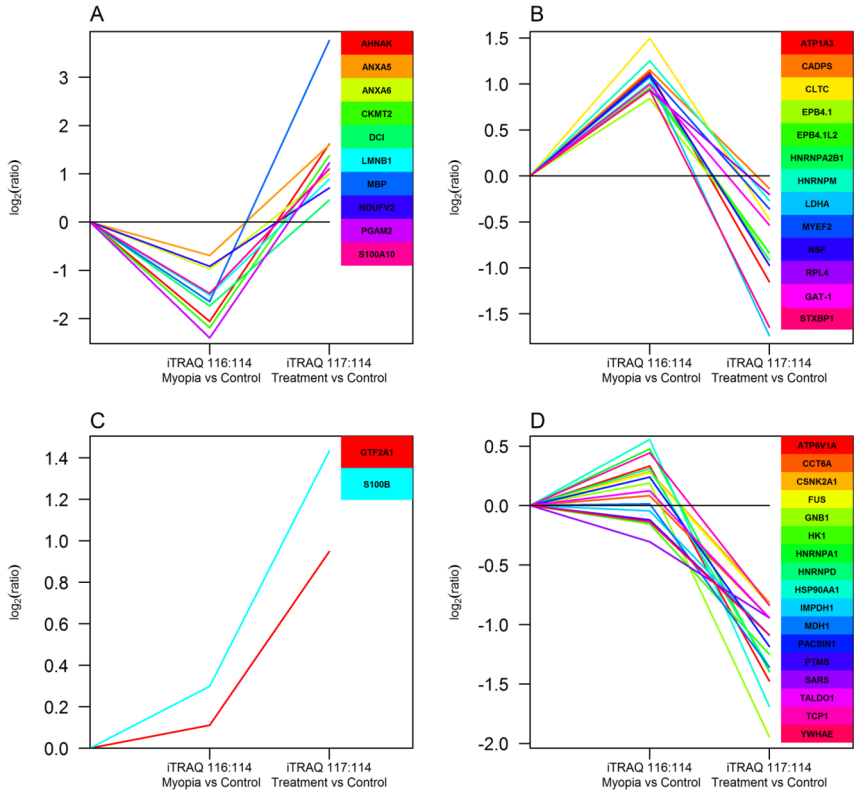

Figure 5. Clustering analysis on up-regulated or down-regulated proteins common to four sets of data showing the similar trend of the expression profile in control, myopia, and atropine treatment using the Short Time-series Expression Miner (STEM) software. (A) Down-regulated in myopia and increased after atropine treatment. (B) Up-regulated in myopia and decreased after atropine treatment. (C) No change in myopia and increased after atropine treatment. (D) No change in myopia and decreased after atropine treatment.

atropine treatment (Figure 5A, Supplement Table 3A in the Supporting Information). Similarly, 10 retina proteins were down-regulated in myopia but gradually showed up-regulation (ratio for treatment/myopia > global mean +1 SD) after atropine treatment (Figure 5B, Supplement Table 3B in the Supporting Information). Additionally, two retina proteins showed no significant changes between myopia and control but up-regulated after atropine treatment (ratio for treatment/myopia > global mean +1 SD, Figure 5C, Supplement Table 3C in the Supporting Information), whereas 17 retina proteins showed no significant changes between myopia and control but down-regulated after atropine treatment (ratio for treatment/myopia < global mean −1 SD, Figure 5D, Supplement Table 3C in the Supporting Information).

Pathway analysis using MetaCore revealed that γ-amino-butyric acid (GABA) is the predominant neurotransmitter regulated in the atropine-treated myopic retina, indicating involvement of GABAergic pathway (Table 2). Detailed analysis of the quantitative proteomics data revealed elevated levels of GABA transporter 1 (GAT-1) in myopic retina ($p = 0.001$) that significantly reduced after atropine treatment ($p = 0.0009$, Figure 6a). Other proteins involved in GABAergic pathway were also identified from this study including NSF (myopia/control ratio: 2.13), Clathrin (myopia/control ratio: 2.82), and Dynein 1 (myopia/control ratio: 2.25) (Supplemental Table 3A in the Supporting Information). These three proteins were up-regulated in myopic eyes as compared with naïve control eyes. NSF and Clathrin also responded to atropine treatment (Supplemental Table 3A in the Supporting Information).

Table 2. Pathway Analysis by MetaCore on 30 Up-Regulated Proteins and 28 Down-Regulated Proteins in Retina from Myopic Group As Compared with Control Group (FDR: false discovery rate)

pathway name	*P* value	FDR
oxidative phosphorylation	4.63×10^{-5}	3.46×10^{-3}
regulation of CFTR activity (normal and CF)	6.79×10^{-5}	3.46×10^{-3}
glycolysis and gluconeogenesis p.3/human version	3.80×10^{-3}	8.15×10^{-2}
glycolysis and gluconeogenesis p.3	3.80×10^{-3}	8.15×10^{-2}
cytoskeleton remodeling_neurofilaments	4.12×10^{-3}	8.15×10^{-2}
neurophysiological process_GABA-A receptor life cycle	4.79×10^{-3}	8.15×10^{-2}
putative pathways for stimulation of fat cell differentiation by bisphenol A	4.69×10^{-3}	8.54×10^{-2}
normal and pathological TGF-beta-mediated regulation of cell proliferation	7.11×10^{-3}	8.54×10^{-2}
development_role of CDK5 in neuronal development	7.53×10^{-3}	8.54×10^{-2}
wtCFTR and deltaF508 traffic/membrane expression (normal and CF)	9.35×10^{-3}	8.67×10^{-2}
glycolysis and gluconeogenesis p. 2/human version	9.35×10^{-3}	8.67×10^{-2}
mitochondrial unsaturated fatty acid beta-oxidation	1.29×10^{-2}	1.10×10^{-1}
some pathways of EMT in cancer cells	1.64×10^{-2}	1.29×10^{-1}
ubiquinone metabolism	3.30×10^{-2}	2.33×10^{-1}
cell adhesion_role of CDK5 in cell adhesion	3.43×10^{-2}	2.33×10^{-1}
DNA damage_role of NFBD1 in DNA damage response	4.92×10^{-2}	2.37×10^{-1}

dx.doi.org/10.1021/pr500558y | J. Proteome Res. 2014, 13, 4647−4658

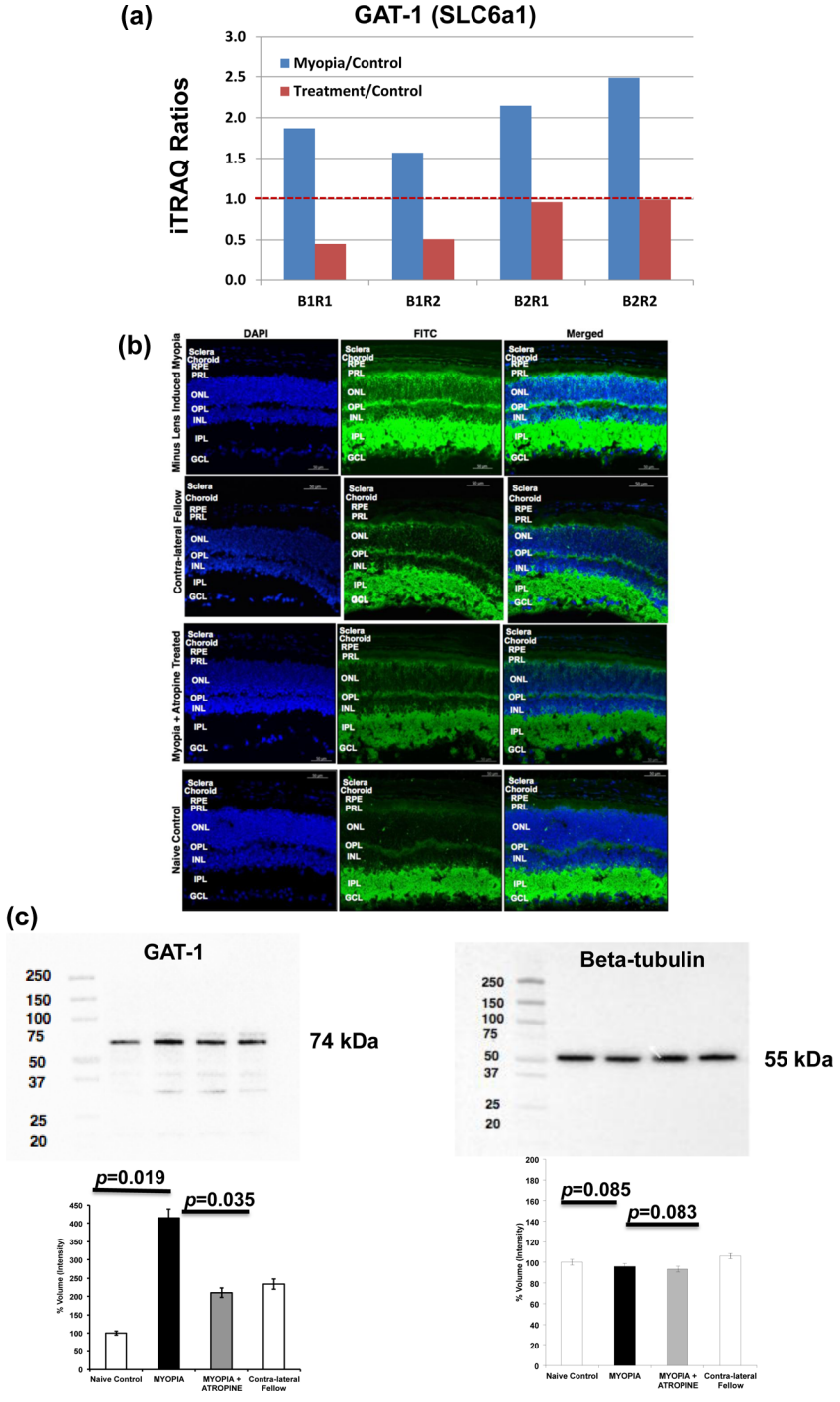

Figure 6. (a) iTRAQ results of GAT-1 level in myopic group and atropine-treated group as compared with control group. (B1R1 and B1R2 represent Batch1, run1 and Batch 1, run2; B2R1 and B2R2 represent Batch2, run1 and Batch 2, run2). Blue bar: Myopia versus control; Red bar: Atropine-treated versus control. (b) Immunofluorescence labeling of GAT-1 in mouse retina, RPE, choroid, and sclera in naïve control and contralateral fellow eyes (exposure time for FITC/DAPI: 800/40Ms), induced myopic eyes (exposure time for FITC/DAPI: 800/60Ms), and atropine-treated eyes (exposure time for FITC/DAPI: 800/110Ms). The fluorescence intensity labeled of the green color shows the localization of proteins, and blue color indicates the nuclei that were stained with DAPI. Lower levels of GAT-1 abundance were seen in atropine-treated retina, RPE, choroid, and sclera similar to naïve control and contralateral fellow, whereas higher levels were observed in myopic retina, RPE, choroid, and sclera. The following abbreviations represent the retinal layers: NFL, nerve fiber layer; GCL, ganglion cell layer; IPL, inner plexiform layer; INL, inner nuclear layer; OPL, outer plexiform layer; ONL, outer nuclear layer; PRL, photoreceptor layer; and RPE, retinal pigment epithelium. $n = 3$ eyes per group and repeated in triplicate. (c) Retinal levels of GABA transporter-1 (GAT-1) in lens-induced myopic, contralateral fellow, atropine treated, and naïve control eyes. Beta-tubulin was used as a loading control. Western blot analysis of GAT-1 proteins in lens-induced myopic, atropine-treated, and naïve control eyes showed a pattern of protein expression similar to that of proteomics analysis. Data represent the mean ± SD; Significance level $p \leq 0.05$.

dx.doi.org/10.1021/pr500558y | J. Proteome Res. 2014, 13, 4647−4658

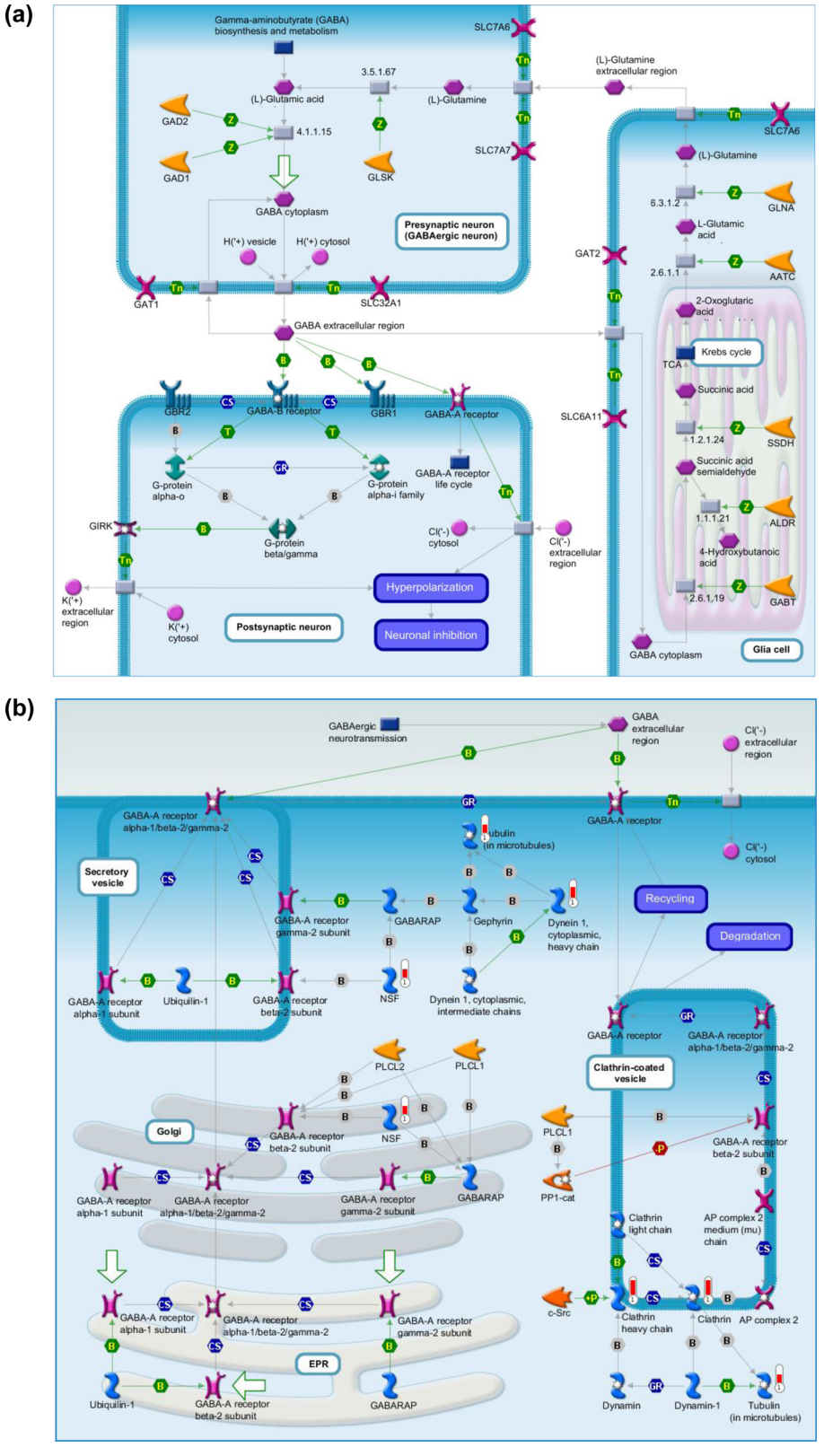

Figure 7. (a,b) Pathway analysis revealed the involvement of GABA pathway using GeneGo MetaCore software.

Validation

Immunofluorescence staining using specific antibody to GAT-1 was used in the mouse retina, RPE, choroid, and scleral tissue to study the localization of GABA transporters in the atropine-treated myopic retinas (Figure 6b). Sections incubated with 4% BSA without primary antibody were used as a negative control. GAT-1 was constitutively present in the inner retina of all groups (naïve control, LIM, atropine-treated, and contralateral fellow). GAT-1 was weakly expressed in the RPE, choroid, and sclera of naïve control, contralateral fellow, and atropine-treated groups.

dx.doi.org/10.1021/pr500558y | J. Proteome Res. 2014, 13, 4647−4658

On the contrary, it was highly expressed in the RPE, choroid, and scleral tissue of the LIM group. Moreover, this was much higher in the myopic inner retina, especially in the ganglion cell layer (GCL).

Western blot was carried out in the myopic, atropine-treated, and naïve control retina to further validate the expression of GAT-1. ß-Tubulin was used as a loading control (Figure 6c). MYEF2 and STBXP1 proteins were also validated (Supplemental Figure 2 in the Supporting Information) in addition to GAT-1. In myopic retina, GAT-1, MYEF2, and STBXP1 protein levels were up-regulated as compared with atropine-treated and naïve control retina.

DISCUSSION

Our results showed for the first time a comprehensive quantitative proteomic data derived from a mouse eye with nearly 4000 unique proteins (FDR < 1%) in the retina. This was evaluated in previously established mouse model of experimental myopia, characterized by axial elongation, refractive error, and sclera remodeling, thus mimicking human myopia.[29] In addition, these mice also respond to the atropine treatment by retarding the progression of myopia.[31]

Relative quantitative proteomic analysis showed a differential expression of retinal proteins in myopic mouse eyes compared with atropine-treated and naïve eyes. In total, 30 retinal proteins were up-regulated and 28 retinal proteins were down-regulated in myopic eyes as compared with control eyes in all four analyses (two biological replicates and two technical replicates). In 30 up-regulated retinal proteins, 13 of them responded to atropine treatment and showed reduced levels. Similarly, in 28 down-regulated retinal proteins, 10 of them appeared to be elevated after atropine treatment. Interestingly, another 19 retinal proteins that exhibited no significant changes between myopic eyes and control eyes showed either up-regulation (2 proteins) or down-regulation (17 proteins) after atropine treatment. Subsequent pathway analysis indicated involvement of GABAergic pathway (Figure 7a) in the development of myopia. In-depth analysis of the quantitative proteomics data suggested modulation of GABA transporter 1 (GAT-1) in response to myopia development and subsequent atropine treatment. LIM eyes showed significantly high levels of GAT-1 expression in the RPE, choroid, sclera, and inner retina, particularly in GCL compared with the atropine-treated or naïve controls (Figure 6b). Apart from GAT-1, other proteins in this GABAergic pathway were also found to be up-regulated, such as, NSF, Clathrin, and Dynein 1 (Figure 7b). In addition to GAT-1, our data show that MYEF2 and STBXP1 proteins were also up-regulated in response to myopia development and restore to normal levels after receiving topical atropine treatment. Previous studies also reported that there was an association of myelinated nerve fibers with axial myopia, which would need further study to understand this mechanism in the development of myopia.[40−42]

Neuronal retinal cells have been reported to be involved in the development of myopia and uncompensated scleral growth. Changes in retinal concentrations of several substances have been demonstrated to be associated with altered eye growth, including dopamine,[43,14] glucagon,[44,45] early growth response factor-1 (EGR1 or ZENK),[46] retinoic acid,[47,48] and vasoactive intestinal peptide (VIP).[49] However, how the retina influences elongation of sclera and the underlying signal molecules or pathways resulting in myopia remains to be seen. Emerging evidence suggest that sclera surrounds the retina and vitreous, and signals from these sources must reach the scleral fibroblasts, which remodel the sclera causing elongation.[50] The sclera is the site of tissue remodeling leading to longitudinal changes, but retinal input has been shown to modulate the growth changes by an as yet unknown mechanism.[43,51] The identification of unique retinal proteins involved in myopia will provide insight into the molecular basis of this eye disorder that will aid in identifying and validating pathways that are involved in eye growth and development.

Atropine, a nonselective muscarinic antagonist, has been reported to inhibit the progression of human myopia probably by neurotransmission involving muscarinic receptors in the sclera.[52] Muscarinic receptors are localized throughout the neural retina, and significant amounts are present in the RPE.[53] Previous studies have shown that atropine inhibits progression of myopia in humans and in experimentally induced myopia in animals, although the mechanisms of action are relatively unknown.[9,31]

The growth of vertebrate eye is controlled by the retinal neurons through biochemical signals controlling scleral growth and thus visual control of the refractive development. The role of these biological signals needs further investigation and could serve as one of the pathways to inhibit the progression of myopia. In the present study, we found several components of the retinal GABAergic pathway that are up-regulated in experimentally induced myopic mouse retina, and chronic administration of atropine was found to restore these levels back to normal. GABA is the major inhibitory neurotransmitter in retina and other parts of the central nervous system.[54,55] It binds to three distinct types of GABAergic receptors: $GABA_A$, $GABA_B$, and $GABA_C$.[56] $GABA_A$ and $GABA_C$ receptors are ligand-gated chloride channels and mediate fast synaptic inhibition when activated by GABA.[57] $GABA_B$ is a metabotropic receptor, which signals through G-proteins and regulates via potassium channels and voltage-gated calcium channels. In contrast with $GABA_A$ and $GABA_C$ receptors, $GABA_B$ receptors mediate slow synaptic inhibition.[58] GABA receptors have been found to be expressed in chick cornea, sclera, and retina,[59−61] but $GABA_C$ receptors are most prominent in the retina. Previous studies suggested that $GABA_C$ receptors have possible roles in myopia, circadian rhythms, sleep-wake behavior, and memory.[16,62,63] Fischer et al.[64] suggested that retinal cholinergic amacrine cells containing acetylcholine, ENK, or VIP are not required for the progression of form-deprived myopia (FDM), however those containing dopamine, GABA, and glucagon may be required. One possibility is that atropine-targeting muscarinic acetylcholine receptors (mAChRs) are located directly on GABAergic neurons. A recent report by Baba et al.[65] indicates that mAChRs on GABAergic neuronal somas/dendrites can enhance GABA release. There is another possibility based on the fact that atropine at low concentrations has an antagonistic action on muscarinic signaling whereas at high concentrations targets GABAergic synaptic transmission in the subfornical organ of rat slice preparations.[66] However, whether high concentrations of atropine affect GABAergic transmission in retina is yet to be determined. Several studies have shown that GABA agonist can directly modulate eye growth, and GABA antagonists inhibit myopia in the chick model;[16,61] however, mechanism and site of action in the retina remain obscure.

Quantitative proteomic analysis using iTRAQ method revealed that components of the GABAergic neurotransmission pathway, GABA transporters such as GAT-1 and to a lesser extent GAT-3, are up-regulated in lens-induced myopic eye. On the contrary, atropine treatment for 28 days in these myopic eyes restored GAT-1 expression back to control retinal levels. Similar trend was also observed for GAT-3 (elevated in myopic retina

with $p = 0.0099$ and reduced after atropine treatment with $p = 0.004$), although its ratio for myopia/control in the first batch (1.39 and 1.47) was slightly below our cutoff value. These results suggest that GABAergic neurotransmitter pathway in the retina might be a potential player in the development or progression of myopia. There are five GABA transporters known including one vesicular GABA transporter (VGAT) and four plasma membrane transporters (GAT-1, GAT-2, GAT-3, and GAT-4).[67] GATs are members of the SLC6 family of proteins that are related to the Na^+/Cl^--dependent neurotransmitter transporter superfamily.[68] They play an important role in terminating the GABAergic transmission by its rapid reuptake into presynaptic neurons and surrounding glial cells.[69] There are notable species differences and inconsistencies in the distribution of GAT's across the retinal tissues.[70] GAT-1 is predominantly localized in neuronal cells including amacrine, displaced amacrine, and ganglion cells. In the present study, immunochemical analysis confirms that component of the GABA transporter GAT-1 is widely distributed throughout the retina and significantly up-regulated in the lens-induced myopic retinas. Atropine treatment to these retinas attenuates expression of GABA transporter toward near normal levels. Increased availability of GABA in the experimentally induced myopic eyes activates GAT's in the retina, which can be counteracted by atropine treatment.

CONCLUSIONS

In conclusion, lens-induced mouse myopic eyes may influence GABAergic neurotransmission by up-regulation of GAT-1 in neural retina, as revealed by quantitative iTRAQ proteomics. Additionally, atropine treatment restores retinal GAT-1 to near-normal levels, supporting the notion that GABAergic signaling system might modulate scleral connective tissue involved in the progression of myopia.

ASSOCIATED CONTENT

Supporting Information

Supplemental Table 1: Complete list of 3882 proteins identified from mouse retina tissue (false discovery rate <1%). Supplemental Table 2: Complete list of over 3000 proteins with iTRAQ quantitative data (Myopia vs Control, Treatment vs Control) in two biological replicates (Batch 1 and Batch 2). Supplemental Table 3: iTRAQ ratios of up-regulated or down-regulated retina proteins in myopic group as compared with control group and those responded to atropine treatment. Supplemental Figure 1: Gene ontology analysis of mouse retina proteome: (A) cellular component, (B) biological process, and (C) molecular function. Supplemental Figure 2: Validation results by Western blot for MEF2 and STXBP1. This material is available free of charge via the Internet at http://pubs.acs.org.

AUTHOR INFORMATION

Corresponding Author

*E-mail: zhou.lei@seri.com.sg. Tel: + (65) 63224546. Fax: + (65) 63224599.

Author Contributions

▽V.A.B. and S.S.C. contributed equally to this work.

Notes

The authors declare no competing financial interest.

ACKNOWLEDGMENTS

This work was supported by grants from the National Medical Research Council, Singapore [NMRC/CG/SERI/T1 & T2/2010, NMRC/CG/SERI/2013, and NMRC/IRG/1117/2008] to V.A.B. and L.Z. We also thank SingHealth Foundation for supporting proteomics core facility. We also acknowledge grants from SingHealth Foundation [R756/40/2010 SHF; R729/13/2010 SHF] to S.S.C., NIG award [R751/35/2010 NMRC] to S.S.C., and Biomedical Research Council, Translational Clinical Research Partnership [TCRP0101672B/R826B & C to V.A.B. and S.S.C.]. NIH grants R01 EY004864, R01 EY016435, R01 EY022342, and P30 EY 006360 and an unrestricted departmental grant from Research to Prevent Blindness, Inc. (RPB). P.M.I. is a recipient of a Senior Scientific Investigator Award from RPB. We also thank Ignatius Chua for the technical assistance in data processing.

REFERENCES

(1) Midelfart, A.; Kinge, B.; Midelfart, S.; Lydersen, S. Prevalence of refractive errors in young and middle-aged adults in Norway. *Acta Ophthalmol. Scand.* **2002**, *80*, 501−505.
(2) Saw, S. M.; Gazzard, G.; Au Eong, K. G.; Tan, D. T. Myopia: attempts to arrest progression. *Br. J. Ophthalmol.* **2002**, *86*, 1306−1311.
(3) Saw, S. M.; Tong, L.; Chua, W. H.; Chia, K. S.; et al. Incidence and progression of myopia in Singaporean school children. *Invest. Ophthalmol. Visual Sci.* **2005**, *46*, 51−57.
(4) Takashima, T.; Yokoyama, T.; Futagami, S.; Ohno-Matsui, K.; et al. The quality of life in patients with pathologic myopia. *Jpn. J. Ophthalmol.* **2001**, *45*, 84−92.
(5) Lin, L. L.; Shih, Y. F.; Hsiao, C. K.; Chen, C. J. Prevalence of myopia in Taiwanese schoolchildren: 1983 to 2000. *Ann. Acad. Med. Singapore* **2004**, *33*, 27−33.
(6) Seet, B.; Wong, T. Y.; Tan, D. T. H.; Saw, S. M.; Balakrishnan, V.; Lee, L. K. H.; Lim, A. S. M. Myopia in Singapore: taking a public health approach. *Br. J. Ophthalmol.* **2001**, *85*, 521−526.
(7) Cooper, J.; Schulman, E.; Jamal, N. Current status on the development and treatment of myopia. *Optometry* **2012**, *83*, 179−199.
(8) Tong, L.; Huang, X. L.; Koh, A. L.; Zhang, X.; Tan, D. T.; Chua, W. H. Atropine for the treatment of childhood myopia: effect on myopia progression after cessation of atropine. *Ophthalmology* **2009**, *116*, 572−579.
(9) Chua, W. H.; Balakrishnan, V.; Chan, Y. H.; Tong, L.; Ling, Y.; Quah, B. L.; Tan, D. Atropine for the treatment of childhood myopia. *Ophthalmology* **2006**, *113*, 2285−2291.
(10) Lee, J. J.; Fang, P. C.; Yang, I. H.; Chen, C. H.; Lin, P. W.; Lin, S. A.; Kuo, H. K.; Wu, P. C. Prevention of myopia progression with 0.05% atropine solution. *J. Ocul. Pharmacol. Ther.* **2006**, *22*, 41−46.
(11) Fan, D. S.; Lam, D. S.; Chan, C. K.; Fan, A. H.; Cheung, E. Y.; Rao, S. K. Topical atropine in retarding myopic progression and axial length growth in children with moderate to severe myopia: a pilot study. *Jpn. J. Ophthalmol.* **2007**, *51*, 27−33.
(12) Chia, A.; Li, W.; Tan, D.; Luu, C. D. Full-field electroretinogram findings in children in the atropine treatment for myopia (ATOM2) study. *Doc. Ophthalmol.* **2013**, *126*, 177−186.
(13) Raviola, E.; Wiesel, T. N. An animal model of myopia. *N. Engl. J. Med.* **1985**, *312*, 1609−1615.
(14) Stone, R. A.; Lin, T.; Laties, A. M.; Iuvone, P. M. Retinal dopamine and form-deprivation myopia. *Proc. Natl. Acad. Sci. U S A* **1989**, *86*, 704−706.
(15) Stone, R. A.; Pardue, M. T.; Iuvone, P. M.; Khurana, T. S. Pharmacology of myopia and potential role for intrinsic retinal circadian rhythms. *Exp. Eye Res.* **2013**, *114*, 35−47.
(16) Stone, R. A.; Liu, J.; Sugimoto, R.; Capehart, C.; Zhu, X.; Pendrak, K. GABA, experimental myopia, and ocular growth in chick. *Invest. Ophthalmol. Visual Sci.* **2003**, *44*, 3933−3946.
(17) Schmid, K. L.; Strasberg, G.; Rayner, C. L.; Hartfield, P. J. The effects and interactions of GABAergic and dopaminergic agents in the

prevention of form deprivation myopia by brief periods of normal vision. *Exp. Eye Res.* **2013**, *110*, 88−95.
(18) Rohrer, B.; Spira, A. W.; Stell, W. K. Apomorphine blocks form-deprivation myopia in chickens by a dopamine D2-receptor mechanism acting in retina or pigmented epithelium. *Vis. Neurosci.* **1993**, *10*, 447−453.
(19) McCarthy, C. S.; Megaw, P.; Devadas, M.; Morgan, I. G. Dopaminergic agents affect the ability of brief periods of normal vision to prevent form-deprivation myopia. *Exp. Eye Res.* **2007**, *84*, 100−107.
(20) Boatright, J. H.; Rubim, N. M.; Iuvone, P. M. Regulation of endogenous dopamine release in amphibian retina by gamma-aminobutyric acid and glycine. *Vis. Neurosci.* **1994**, *11*, 1003−1012.
(21) Gustincich, S.; Feigenspan, A.; Wu, D. K.; Koopman, L. J.; Raviola, E. Control of dopamine release in the retina: A transgenic approach to neural networks. *Neuron* **1997**, *18* (5), 723−736.
(22) Lam, T. C.; Li, K. K.; Lo, S. C.; Guggenheim, J. A.; To, C. H. A chick retinal proteome database and differential retinal protein expressions during early ocular development. *J. Proteome Res.* **2006**, *5*, 771−784.
(23) Lam, T. C., Li, K. K., Lo, S. C., Guggenheim, J. A., To, C. H., Application of fluorescence difference gel electrophoresis technology in searching for protein biomarkers in chick myopia. *J. Proteome Res. 6*, 4135−4149.
(24) Gao, H.; Frost, M. R.; Siegwart, J. T., Jr.; Norton, T. T. Patterns of mRNA and protein expression during minus-lens compensation and recovery in tree shrew sclera. *Mol. Vis.* **2011**, *17*, 903−919.
(25) Frost, M. R.; Norton, T. T. Alterations in protein expression in tree shrew sclera during development of lens-induced myopia and recovery. *Invest. Ophthalmol. Visual Sci.* **2012**, *53*, 322−336.
(26) Jostrup, R.; Shen, W.; Burrows, J. T.; Sivak, J. G.; et al. Identification of myopia-related marker proteins in tilapia retinal, RPE, and choroidal tissue following induced form deprivation. *Curr. Eye Res.* **2009**, *34*, 966−975.
(27) Zhou, X.; Ye, J.; Willcox, M. D.; Xie, R.; et al. Changes in protein profiles of guinea pig sclera during development of form deprivation myopia and recovery. *Mol. Vis.* **2010**, *16*, 2163−2174.
(28) Duan, X.; Lu, Q.; Xue, P.; Zhang, H.; et al. Proteomic analysis of aqueous humor from patients with myopia. *Mol. Vis.* **2008**, *14*, 370−377.
(29) Barathi, V. A.; Boopathi, V. G.; Yap, E. P.; Beuerman, R. W. Two models of experimental myopia in the mouse. *Vision Res.* **2008**, *48*, 904−916.
(30) Barathi, V. A.; Beuerman, R. W.; Schaeffel, F. Effects of unilateral topical atropine on binocular pupil responses and eye growth in mice. *Vision Res.* **2009**, *49*, 383−387.
(31) Barathi, V. A.; Beuerman, R. W. Molecular mechanisms of muscarinic receptors in mouse scleral fibroblasts: Prior to and after induction of experimental myopia with atropine treatment. *Mol. Vis.* **2011**, *17*, 680−692.
(32) Barathi, V. A.; Kwan, J. L.; Tan, Q. S.; Weon, S. R.; Seet, L. F.; Goh, L. K.; Vithana, E. N.; Beuerman, R. W. Muscarinic cholinergic receptor (M2) plays a crucial role in the development of myopia in mice. *Dis. Models & Mech.* **2013**, *6* (5), 1146−1158.
(33) Patel, N.; Solanki, E.; Picciani, R.; Cavett, V.; Caldwell-Busby, J. A.; Bhattacharya, S. K. Strategies to recover proteins from ocular tissues for proteomics. *Proteomics* **2008 Mar**, *8* (5), 1055−1070.
(34) Huang da, W.; Sherman, B. T.; Lempicki, R. A. Systematic and integrative analysis of large gene lists using DAVID bioinformatics resources. *Nat. Protoc.* **2009**, *4*, 44−57.
(35) Huang da, W.; Sherman, B. T.; Lempicki, R. A. Bioinformatics enrichment tools: paths toward the comprehensive functional analysis of large gene lists. *Nucleic Acids Res.* **2009**, *37*, 1−13.
(36) Ernst, J.; Bar-Joseph, Z. STEM: a tool for the analysis of short time series gene expression data. *BMC Bioinf.* **2006**, *7*, 191.
(37) Schaeffel, F.; Burkhardt, E.; Howland, H. C.; Williams, R. W. Measurement of refractive state and deprivation myopia in two strains of mice. *Opt. Vis. Sci.* **2004**, *81*, 99−110.
(38) Hill, E. G.; Schwacke, J. H.; Comte-Walters, S.; Slate, E. H.; Oberg, A. L.; Eckel-Passow, J. E.; Therneau, T. M.; Schey, K. L. A statistical model for iTRAQ data analysis. *J. Proteome Res.* **2008**, *7* (8), 3091−3101.
(39) Ross, P. L.; Huang, Y. N.; Marchese, J. N.; Williamson, B.; Parker, K.; Hattan, S.; Khainovski, N.; Pillai, S.; Dey, S.; Daniels, S.; Purkayastha, S.; Juhasz, P.; Martin, S.; Bartlet-Jones, M.; He, F.; Jacobson, A.; Pappin, D. J. Multiplexed protein quantitation in Saccharomyces cerevisiae using amine-reactive isobaric tagging reagents. *Mol. Cell. Proteomics* **2004**, *3* (12), 1154−1169.
(40) Weiss, A. H. Unilateral high myopia: optical components, associated factors, and visual outcomes. *Br. J. Ophthalmol.* **2003 Aug**, *87* (8), 1025−1031.
(41) Hittner, H. M.; Antosyzk, J. H. Unilateral peripapilary myelinated nerve fibers with myopia and/or amblyopia. *Arch. Ophthalmol.* **1987**, *105*, 943−948.
(42) Ellis, G. S.; Frey, T.; Gouterman, R. Z. Myelinated nerve fibers, axial myopia and refractory amblyopia: an organic disease. *J. Pediatr. Ophthalmol. Strabismus* **1987**, *24*, 111−119.
(43) Feldkaemper, M.; Schaeffel, F. An updated view on the role of dopamine in myopia. *Exp. Eye Res.* **2013**, *114*, 106−119.
(44) Vessey, K. A.; Lencses, K. A.; Rushforth, D. A.; Hruby, V. J.; Stell, W. K. Glucagon receptor agonists and antagonists affect the growth of the chick eye: a role for glucagonergic regulation of emmetropization? *Invest. Ophthalmol. Visual Sci.* **2005**, *46*, 3922−3931.
(45) Buck, C.; Schaeffel, F.; Simon, P.; Feldkaemper, M. Effects of positive and negative lens treatment on retinal and choroidal glucagon and glucagon receptor mRNA levels in the chicken. *Invest. Ophthalmol. Visual Sci.* **2004**, *45*, 402−409.
(46) Fischer, A. J.; McGuire, J. J.; Schaeffel, F.; Stell, W. K. Light- and focus-dependent expression of the transcription factor ZENK in the chick retina. *Nat. Neurosci.* **1999**, *2*, 706−712.
(47) Seko, Y.; Shimokawa, H.; Tokoro, T. In vivo and in vitro association of retinoic acid with form-deprivation myopia in the chick. *Exp. Eye Res.* **1996**, *63*, 443−452.
(48) Mertz, J. R.; Wallman, J. Choroidal retinoic acid synthesis: a possible mediator between refractive error and compensatory eye growth. *Exp. Eye Res.* **2000**, *70*, 519−527.
(49) Brand, C.; Burkhardt, E.; Schaeffel, F.; Choi, J. W.; Feldkaemper, M. P. Regulation of Egr-1, VIP, and Shh mRNA and Egr-1 protein in the mouse retina by light and image quality. *Mol. Vis.* **2005**, *11*, 309−320.
(50) Frost, M. R.; Norton, T. T. Alterations in protein expression in tree shrew sclera during development of lens-induced myopia and recovery. *Invest. Ophthalmol. Visual Sci.* **2012**, *53*, 322−336.
(51) Stone, R. A.; Lin, T.; Iuvone, P. M.; Laties, A. M. Postnatal control of ocular growth: dopaminergic mechanisms. *Ciba Found. Symp.* **1990**, *155*, 45−62.
(52) Mitchelson, F. Muscarinic receptor agonists and antagonists: effects on ocular function. *Handb. Exp. Pharmacol.* **2012**, *208*, 263−298.
(53) Barathi, V. A.; Weon, S. R.; Rebekah, P. W. Y.; Beuerman, R. W. Muscarinic regulation of epidermal growth factor receptor in mammalian retinal pigment epithelial (RPE) cells. Invest. *Ophthalmol. Vis. Sci.* **2008**, *49* (Suppl,), 3535.
(54) Fagiolini, M.; Fritschy, J. M.; Low, K.; Mohler, H.; Rudolph, U.; et al. Specific GABAA circuits for visual cortical plasticity. *Science* **2004**, *303*, 1681−1683.
(55) Akerman, C. J.; Cline, H. T. Refining the roles of GABAergic signaling during neural circuit formation. *Trends Neurosci.* **2007**, *30*, 382−389.
(56) Froestl, W. Chemistry and pharmacology of GABAB receptor ligands. *Adv. Pharmacol.* **2010**, *58*, 19−62.
(57) Chebib, M.; Johnston, G. A. GABA-activated ion channels: medicinal chemistry and molecular biology. *J. Med. Chem.* **2000**, *43*, 1427−1447.
(58) Marshall, F. H.; Jones, K. A.; Kaupmann, K.; Bettler, B. GABAB receptors − the first 7TM heterodimers. *Trends Pharmacol. Sci.* **1999**, *20*, 396−399.
(59) Cheng, Z. Y.; Chebib, M.; Schmid, K. L. Identification of GABA receptors in chick cornea. *Mol. Vis.* **2012**, *18*, 1107−1114.
(60) Cheng, Z. Y.; Chebib, M.; Schmid, K. L. ρ1 GABAC receptors are expressed in fibrous and cartilaginous layers of chick sclera and located

on sclera fibroblasts and chondrocytes. *J. Neurochem.* **2011**, *118*, 281−287.
(61) Chebib, M.; Hinton, T.; Schmid, K. L.; et al. Novel, potent, and selective GABAC antagonists inhibit myopia development and facilitate learning and memory. *J. Pharmacol. Exp. Ther.* **2009**, *328*, 448−457.
(62) Arnaud, C.; Gauthier, P.; Gottesmann, C. Study of a GABAC receptor antagonist on sleep-waking behavior in rats. *Psychopharmacology* **2001**, *154*, 415−419.
(63) Gibbs, M. E.; Johnston, G. A. Opposing roles for GABAA and GABAC receptors in short-term memory formation in young chicks. *Neuroscience* **2005**, *131*, 567−576.
(64) Fischer, A. J.; Miethke, P.; Morgan, I. G.; Stell, W. K. Cholinergic amacrine cells are not required for the progression and atropine-mediated suppression of form-deprivation myopia. *Brain Res.* **1998**, *794*, 48−60.
(65) Baba, H.; Kohno, T.; Okamoto, M.; Goldstein, P. A.; Shimoji, K.; Yoshimura, M. Muscarinic facilitation of GABA release in substantia gelatinosa of the rat spinal dorsal horn. *J. Physiol. (London, U. K.)* **1998**, *508*, 83−93.
(66) Xu, S. H.; Ono, K.; Honda, E.; Inenaga, K. Noncholinergic actions of atropine on GABAergic synaptic transmission in the subfornical organ of rat slice preparations. *Toxicol. Appl. Pharmacol.* **2002**, *178*, 180−185.
(67) Sałat, K.; Kulig, K. GABA transporters as targets for new drugs. *Future Med. Chem.* **2011**, *3*, 211−222.
(68) Kleppner, S. R.; Tobin, A. J. *Encyclopedia of the Human Brain*; Ramachandran, V. S., Ed.; Academic Press: New York, 2002; pp 353−367. http://www.sciencedirect.com/science/article/pii/B0122272102001503.
(69) Wood, D.; Sidhu, H. S. A comparative study and partial characterization of multi-uptake systems for gamma-aminobutyric acid. *J. Neurochem.* **1987**, *49*, 1202.
(70) Honda, S.; Yamamoto, M.; Saito, N. Immunocytochemical localization of three subtypes of GABA transporter in rat retina. *Mol. Brain Res.* **1995**, *33*, 319−325.